Received: 30 December 2023 | Accepted: 18 July 2024

DOI: 10.1111/pce.15068

ORIGINAL ARTICLE

Plant, Cell & Environment PC&E WILEY

Photosynthetic capacity in middle-aged larch and spruce acclimates independently to experimental warming and elevated CO_2

Mirindi Eric Dusenge[1,2] | Jeffrey M. Warren[3] | Peter B. Reich[4,5,6] | Eric J. Ward[7] | Bridget K. Murphy[2,8,9] | Artur Stefanski[5] | Raimundo Bermudez[5] | Marisol Cruz[10] | David A. McLennan[3] | Anthony W. King[3] | Rebecca A. Montgomery[5] | Paul J. Hanson[3] | Danielle A. Way[2,11,12,13]

[1]Department of Biology, Mount Allison University, Sackville, New Brunswick, Canada

[2]Department of Biology, The University of Western Ontario, London, Ontario, Canada

[3]Climate Change Science Institute and Environmental Sciences Division, Oak Ridge National Laboratory, Oak Ridge, Tennessee, USA

[4]Institute for Global Change Biology, and School for the Environment and Sustainability, University of Michigan, Ann Arbor, Michigan, USA

[5]Department of Forest Resources, University of Minnesota, Saint Paul, Minnesota, USA

[6]Hawkesbury Institute for the Environment, University of Western Sydney, Penrith, New South Wales, Australia

[7]Earth System Science Interdisciplinary Center, University of Maryland, College Park, Maryland, USA

[8]Department of Biology, University of Toronto Mississauga, Mississauga, Ontario, Canada

[9]Graduate Program in Cell and Systems Biology, University of Toronto, Toronto, Ontario, Canada

[10]Departamento de Ciencias Biologicas, Universidad de Los Andes, Bogota, Colombia

[11]Division of Plant Sciences, Research School of Biology, The Australian National University, Canberra, Australia

[12]Nicholas School of the Environment, Duke University, Durham, North Carolina, USA

[13]Environmental and Climate Sciences Department, Brookhaven National Laboratory, Upton, New York, USA

Correspondence

Mirindi Eric Dusenge, Department of Biology, Mt Allison University, Sackville, New Brunswick, E4L 1E4, Canada.
Email: mdusenge@mta.ca

Danielle A. Way, Department of Biology, The University of Western Ontario, London, Ontario, N6A 3K7, Canada.
Email: danielle.way@anu.edu.au

Funding information

NSERC Discovery and Strategic programs, Grant/Award Numbers: RGPIN/04677-2019, STPGP/521445-2018; U.S. NSF Biological Integration Institutes, Grant/Award Number: DBI-2021898; USGS Climate Research and

Abstract

Photosynthetic acclimation to both warming and elevated CO_2 of boreal trees remains a key uncertainty in modelling the response of photosynthesis to future climates. We investigated the impact of increased growth temperature and elevated CO_2 on photosynthetic capacity (V_{cmax} and J_{max}) in mature trees of two North American boreal conifers, tamarack and black spruce. We show that V_{cmax} and J_{max} at a standard temperature of 25°C did not change with warming, while V_{cmax} and J_{max} at their thermal optima (T_{opt}) and growth temperature (T_g) increased. Moreover, V_{cmax} and J_{max} at either 25°C, T_{opt} or T_g decreased with elevated CO_2. The J_{max}/V_{cmax} ratio decreased with warming when assessed at both T_{opt} and T_g but did not

Any use of trade, firm, or product names is for descriptive purposes only and does not imply endorsement by the U.S. Government.

Development Program; Biological and Environmental Research Program in the Office of Science, U.S. Department of Energy

significantly vary at 25°C. The J_{max}/V_{cmax} increased with elevated CO_2 at either reference temperature. We found no significant interaction between warming and elevated CO_2 on all traits. If this lack of interaction between warming and elevated CO_2 on the V_{cmax}, J_{max} and J_{max}/V_{cmax} ratio is a general trend, it would have significant implications for improving photosynthesis representation in vegetation models. However, future research is required to investigate the widespread nature of this response in a larger number of species and biomes.

KEYWORDS

acclimation, black spruce, boreal conifers, SPRUCE project, tamarack, temperature

1 | INTRODUCTION

Boreal forests represent a key component within the global carbon cycle as, through photosynthesis, they absorb a significant amount of carbon from the atmosphere annually (Beer et al., 2010; Houghton, 2007). Accurate representation of photosynthesis of boreal forests within terrestrial biosphere models (TBMs) is, therefore, important to reliably predict both current and future global carbon cycling and associated climatic conditions (Rogers et al., 2022). The boreal region has already warmed more than twice than the global average (IPCC, 2013), and predictions suggest that some regions could potentially warm by 6°C by 2100 compared to a global mean of ~4°C (IPCC, 2021). The Farquhar–von Caemmerer–Berry (FvCB; Farquhar et al., 1980) model of C_3 photosynthesis is widely used to derive the two key parameters representing underlying biochemical processes of photosynthesis, the maximum rate of Rubisco carboxylation (V_{cmax}) and the maximum rate of electron transport (J_{max}) (Farquhar et al., 1980; von Caemmerer, 2000; Wullschleger, 1993). The V_{cmax} and J_{max} are key parameters in many TBMs to simulate current and future terrestrial carbon uptake and sequestration (Knauer et al., 2023; Mercado et al., 2018; Oliver et al., 2022; Rogers, Serbin, et al., 2017; Rogers, 2014). However, many of the TBMs do not currently incorporate long-term acclimation responses of both V_{cmax} and J_{max} to climate change variables such as warming and elevated CO_2 (and their combination) (Lombardozzi et al., 2015; Rogers, Serbin, et al., 2017, 2022; Smith & Dukes, 2013), largely due to the lack of these data and particularly for the boreal region (Rogers et al., 2022; Stinziano et al., 2019). Such a knowledge gap limits the ability of these models to reliably forecast the feedback between boreal forest carbon cycling and future climate.

The least-cost framework (Prentice et al., 2014; Smith et al., 2019) was recently used to predict acclimation of photosynthetic capacity (V_{cmax} and J_{max}) to warming and elevated CO_2 from first-principles (Jiang et al., 2020; Smith & Keenan, 2020; Wang et al., 2020). This framework suggests that V_{cmax} and J_{max} when measured at a given standard temperature (e.g., 25°C) should decrease in warm-grown plants compared to cool-grown counterparts as plants operating in warm growth conditions can achieve optimal carbon assimilation rates with relatively lower photosynthetic protein content (e.g., Rubisco and chlorophylls) (Lu et al., 2020; Maire et al., 2012; Wang et al., 2020; Yamori et al., 2014). But when assessed at growth temperature (T_g), both V_{cmax} and J_{max} should increase with growth temperature but with a lower slope compared to the short-term temperature responses (Smith et al., 2019; Smith & Keenan, 2020; Wang et al., 2020). However, V_{cmax} should increase more strongly than J_{max} with growth temperature due to a greater allocation of resources to Rubisco carboxylation compared to electron transport, as a mechanism to counteract increase in photorespiration associated with rising temperatures (Smith & Keenan, 2020). Therefore, this higher investment in Rubisco carboxylation should lead to a decrease in the J_{max}/V_{cmax} ratio with rising in growth temperature (Smith & Keenan, 2020). Similarly, plants grown under elevated CO_2 conditions should reduce V_{cmax} and Rubisco content since under elevated CO_2 conditions Rubisco is less limited by substrate availability (i.e., CO_2), and thus high carbon assimilation rates can be achieved with relatively lower Rubisco protein content compared to ambient CO_2-grown plants (Smith & Keenan, 2020). In contrast to V_{cmax}, the least-cost framework predicts slightly higher rates of J_{max} with elevated CO_2 which should lead to higher J_{max}/V_{cmax} ratio in elevated CO_2-grown plants compared to ambient CO_2-grown counterparts (Smith & Keenan, 2020).

In the literature, the acclimation responses of photosynthetic capacity to warming are mixed and thus partly disagree with the least-cost optimality theory of photosynthetic capacity. Most previous meta-analyses using both warming experiments and studies with seasonal/spatial natural temperature variability largely indicate a lack of change of V_{cmax} (Kattge & Knorr, 2007; Kumarathunge et al., 2019; Way & Oren, 2010; Crous et al., 2022) and J_{max} (Kattge & Knorr, 2007; Way & Oren, 2010) at a reference temperature of 25°C to increasing growth temperature, with a few exceptions in some datasets reporting a decrease in either V_{cmax25} (Wang et al., 2020) or J_{max25} (Crous et al., 2022; Kumarathunge et al., 2019). However, when measured at prevailing growth temperatures both V_{cmax} and J_{max} consistently increase (Scafaro et al., 2017; Smith & Dukes, 2017; Smith & Keenan, 2020; Way & Oren, 2010), and the J_{max}/V_{cmax} ratio commonly decreases with warming (Crous et al., 2022; Kattge & Knorr, 2007; Kumarathunge et al., 2019; Smith & Dukes, 2017). Similarly, warming responses of photosynthetic capacity rates at a

common temperature in boreal tree species are mixed. In controlled greenhouse/glasshouse experiments on seedlings, V_{cmax} and J_{max} at a standard temperature decreased with warming (Way & Sage, 2008a, 2008b; Dusenge, Madhavji, et al., 2020) but not in (Murphy & Way, 2021), while experimental studies with freely-rooted boreal juvenile (Bermudez et al., 2021; Stefanski et al., 2020) and mature (Lamba et al., 2018) mainly reported no change in V_{cmax} and J_{max}. When measured at growth temperature, V_{cmax} increased in response to warming but not for J_{max} (Murphy & Way, 2021), and the J_{max}/V_{cmax} ratio generally decreases with warming in some studies (Dusenge, Madhavji, et al., 2020; Stefanski et al., 2020; ; Bermudez et al., 2021; Murphy & Way, 2021). However, there are still limited studies that have investigated the response of photosynthetic capacity to warming in mature trees naturally growing in the field.

The acclimation responses of V_{cmax} to long-term exposure to elevated CO_2 is similar to that predicted by the least-cost optimality model, with V_{cmax} decreasing in elevated-CO_2 grown plants compared to ambient CO_2-grown counterparts (Ainsworth & Long, 2005; Leakey et al., 2009; Smith & Keenan, 2020). However, the acclimation responses of J_{max} to elevated CO_2 vary between empirical observations and predictions based on least-cost optimality. Empirical studies commonly reported a decrease in J_{max} with elevated CO_2 (Ainsworth & Long, 2005; Leakey et al., 2009), while the least-cost theory predicts no change or even slightly positive responses (Smith & Keenan, 2020). These differential responses between V_{cmax} and J_{max} result in the J_{max}/V_{cmax} ratio being less positive than predicted by optimality (Smith & Keenan, 2020). Studies conducted on boreal tree species reported mixed responses. The majority of studies, which focused on seedlings in controlled growth conditions, reported a lack of acclimation of V_{cmax} and J_{max} to elevated CO_2 (Dusenge, Madhavji, et al., 2020; Kellomaki & Wang, 1996; Murphy & Way, 2021; Ofori-Amanfo et al., 2020; Wang, 1996). However, two other studies—one examining both V_{cmax} and J_{max} in seedlings (Bigras & Bertrand, 2006) and another focusing solely on V_{cmax} in mature Norway spruce (Lamba et al., 2018)—found strong acclimation of these parameters to elevated CO_2. However, more studies investigating the impact of elevated CO_2 on V_{cmax} and J_{max} in boreal mature trees in the field are still needed.

Given that ongoing climate warming is primarily driven by rising atmospheric CO_2 concentration, it is imperative to examine their combined impacts on V_{cmax} and J_{max} to improve further the predictive capability of TBMs (Dusenge et al., 2019; Norby & Luo, 2004; Smith & Dukes, 2013). However, no study has evaluated predictions of the least-cost optimality theory under warming and elevated CO_2. The main reason is that there are far fewer studies examining the potential interactive effects of warming and elevated CO_2 on V_{cmax} and J_{max}, limiting the theory's validation (Smith & Keenan, 2020). Nevertheless, utilizing the least-cost optimality approach, Smith and Keenan (2020) predicted the response of photosynthetic nitrogen as the sum of simulated nitrogen invested into Rubisco and bioenergetics. Photosynthetic nitrogen concentration can be used as a proxy for rates of V_{cmax} and J_{max} at a standard temperature, as they indirectly reflect the active photosynthetic protein content (Ellsworth et al., 2022; Rogers, 2014). Smith and Keenan's (2020) predictions showed that photosynthetic nitrogen decreased with both warming and elevated CO_2, but growth temperature did not affect the slope of response to elevated CO_2. These predictions suggest that the responses of V_{cmax} and J_{max} rates to atmospheric CO_2 levels will not be significantly influenced by growth temperature.

Results from the few studies that explore the combined effects of warming and elevated CO_2 are largely derived from highly controlled experiments on seedlings, and their findings are mixed, making it challenging to draw consistent conclusions. Some of these studies showed that V_{cmax} and J_{max} at a standard temperature only acclimate to warming but not elevated CO_2 (Crous et al., 2013; Dusenge, Madhavji, et al., 2020; Ghannoum et al., 2010; Kellomaki & Wang, 1996), acclimated to elevated CO_2 but not to warming (Fauset et al., 2019; Ghannoum et al., 2010; Lamba et al., 2018), or no acclimation to any of these two environmental factors (Murphy & Way, 2021; Wang, 1996). The remaining set of studies exposed seedlings to only combined warming and elevated CO_2 without including treatments of their separate effects (e.g., either warming or elevated CO_2), limiting the assessment of potential interactive effects. This latter category of studies demonstrated that seedlings grown under both warming and elevated CO_2 showed decreased V_{cmax} and J_{max} compared to control (both ambient CO_2 and temperature) tree species (Slot et al., 2021; Wang et al., 2022, 2023, 2024). However, there is a need for more data on the responses of V_{cmax} and J_{max} to warming and elevated CO_2, especially in mature trees growing naturally in the field, while also separately manipulating these two factors to explore their potential interactive effects.

With the goal to improve our understanding on how photosynthesis in North America's boreal forests respond to combined warming and elevated CO_2, we assessed the responses of rates of both V_{cmax} and J_{max} to 2 years of warming combined with 1 year of elevated CO_2 in two canopy tree species, black spruce (*Picea mariana*) and tamarack (*Larix laricina*), growing in the field at the southern range of their natural distribution. This study is part of the Spruce and Peatland Responses Under Changing Environments (SPRUCE; https://mnspruce.ornl.gov) long-term experiment, which uses whole-ecosystem heating, spanning from 3 m belowground up to 7 m aboveground using large octagonal open-top enclosures (Hanson et al., 2017). We recently published a companion study (Dusenge et al., 2023) detailing the response of the thermal optima of net photosynthesis (T_{optA}), V_{cmax} (T_{optV}) and J_{max} (T_{optJ}) to warming and elevated CO_2, and rates of net photosynthesis at their respective prevailing growth conditions (A_g). In summary, we found that the T_{optA} of both species increased with warming. However, these increases were not proportional to the warming, as T_{optA} only rose by 0.26–0.35°C per 1°C of warming. Interestingly, these small shifts in T_{optA} were largely influenced by concurrent changes in T_{optV} and T_{optJ}. Furthermore, A_g increased with warming in elevated CO_2 black spruce, while remaining relatively constant in ambient CO_2-grown black spruce and in both ambient and elevated CO_2-grown tamarack with warming. Our current study delves into the detailed responses

of the rates of the photosynthetic biochemical processes, V_{cmax} and J_{max}, aiming to provide further insight into the observed rates of net photosynthesis in the SPRUCE experiment after 2 years of treatments. Based on both the least-cost optimality theory and previous research, the following four hypothesized predictions were tested:

H1. At a standard temperature, photosynthetic capacity (V_{cmax} and J_{max}) will decrease with warming but will increase with growth temperature.

H2. At a standard temperature, photosynthetic capacity will be lower in plants grown under elevated CO_2 conditions compared to those grown under ambient CO_2 conditions.

H3. Photosynthetic capacity will be lower in trees exposed to both warm and elevated CO_2 conditions with comparable responses to their independent effects.

2 | MATERIALS AND METHODS

2.1 | Site description and experimental design

The current study was conducted at the Oak Ridge National Laboratory's SPRUCE project site located at the U.S. Forest Service's Marcell Experimental Forest, in Minnesota, USA (47°30.476′ N; 93°27.162′ W). At the SPRUCE site, the dominant tree species is *Picea mariana* (black spruce) mixed with less abundant *Larix laricina* (tamarack). The SPRUCE experiment uses five temperature treatments (ambient or +0, which serves also as the control, +2.25°C, +4.5°C, +6.75°C, and +9°C above the ambient) established in a regression-based design (Hanson et al., 2017). These temperature treatment levels are controlled within 10 large octagonal open-top enclosures with an interior surface area of 114.8 m^2, and a sampling area of 66.4 m^2. In addition to the temperature treatments, there are also elevated CO_2 treatments, with five enclosures exposed to an ambient-CO_2 atmosphere, while the other five have an elevated CO_2 atmosphere that range between +430 and 500 ppm above the ambient. The whole-ecosystem warming treatments were initiated 15 August 2015, while the CO_2 treatments were introduced a year later, on 15 June 2016. Overall, the targets of the temperature treatment levels and CO_2 concentrations were successfully achieved (Supporting Information S1: Figure S1).

2.2 | Plant material sampling and gas exchange measurements

The data used in this study were conducted between 18–30 June and 15–30 August 2017. The daytime temperatures (4:00–20:30) recorded by a climate station established at the SPRUCE site were 18.97°C and 18.02°C, for June and August, respectively. We studied individuals of 1.9–7.6 m height of the two mixed-age (up to ~45 years old) canopy tree species, black spruce and tamarack. For black spruce, one branchlet of each tree and in each plot was collected and 1-year old needle cohorts (i.e., developed in 2016) from each branchlet was measured. For tamarack, fully expanded current year foliage (i.e., developed in 2017) was used. In the June field campaign, three trees in each plot were sampled, but we decided to reduce the number of harvested branches down to two trees in the August campaign, to reduce the damage that may be caused by overharvesting in this long-term experiment. For tamarack, the same number of branchlets from different trees in each plot was used, except in one plot (in ambient CO_2 and +0) where there was only one tamarack tree to be sampled. All the data were collected on sun-exposed branchlets cut using a pruning pole. After cutting, branchlets were placed in water, and recut under water to avoid xylem transport disruption and stomatal closure.

The collection of branches took place during the early morning hours, specifically between 4 and 5 am on the day of measurement. Subsequently, these branches were carefully placed in water-filled containers within a plastic cooler. They were then transported from the field site located in Marcell, Minnesota to specialized walk-in growth chambers situated at the University of Minnesota in St. Paul, where the subsequent measurements were carried out. Before starting the measurements, branchlets were re-cut again under water. It has been demonstrated that the impact of cutting and the duration between cutting and gas exchange measurements do not exert a significant influence on stomatal conductance in conifers (Akalusi et al., 2021; Dang et al., 1997). Between 10:00 and 20:00 during the June and August field campaigns, seven portable photosynthesis systems (Li-COR 6400 XT, 6400-18 RGB light source, and 6400-22 opaque conifer chamber; LI-COR Biosciences) were employed to carry out gas exchange measurements. Measurements of net CO_2 assimilation rates (A) were conducted under saturating light conditions at 1800 µmol m^{-2} s^{-1}, with variations in air CO_2 concentrations performed sequentially (400, 300, 200, 50, 400, 500, 600, 800, 1200, 1600, and 2000 µmol mol^{-1}) to generate A–C_i curves. These A–C_i curves were conducted at five different leaf temperatures (T_{leaf}) in the following order: 15°C, 25°C, 32.5°C, 40°C and 45°C, which produced 96A – C_i temperature response curves after data quality checks (Dusenge, Ward, et al., 2020). To attain the desired T_{leaf} for each target, we conducted all measurements within a walk-in chamber. This setup ensured that both the entire branch and the Li-COR IRGA (Infrared Gas Analyser) sensor were exposed to the specified temperature for a minimum of 30 min before start-up measurements at that particular temperature. In addition, this approach effectively reduced measurement errors caused by the internal thermal gradient which occurs when the Li-COR and the leaves are exposed to different temperatures, a phenomenon that had been previously documented with LI-6400 instruments (Garen et al., 2022).

Following the gas exchange measurements, we utilized ImageJ software (NH) to calculate the projected leaf area of the sampled needles. Subsequently, we adjusted for the needle area before

conducting the analyses of the gas exchange data. Furthermore, we examined the collected needle tissues for elemental nitrogen concentrations (*N*) using equipment from Costech Analytical Technologies, Inc.

2.3 | Parameterization of photosynthetic capacity

To parameterize V_{cmax} and J_{max} from the A–C_i curves, we used the FvCB (Farquhar, von Caemmerer, and Berry) C_3 photosynthesis model (Farquhar et al., 1980) using Equations (1), (2) and (3) embedded within the *fitacis* function from the 'plantecophys' R package (Duursma, 2015) and with the *bilinear* fitting method:

$$A_c = \frac{V_{cmax}(C_i - \Gamma^*)}{\left[C_i + K_c\left(1 + \frac{O}{K_O}\right)\right]} - R_{day}, \quad (1)$$

where O the intercellular concentrations of O_2, K_c and K_o are the Michaelis–Menten coefficients of Rubisco activity for CO_2 and O_2, respectively, and Γ^* is the CO_2 compensation point in the absence of mitochondrial respiration, and R_{day} is the mitochondrial respiration during light conditions:

$$A_j = \left(\frac{J_{max}}{4}\right) \times \frac{(C_i - \Gamma^*)}{(C_i + 2\Gamma^*)} - R_{day}, \quad (2)$$

$$A_{TPU} = 3TPU, \quad (3)$$

where TPU stands for triose phosphate use.

We kept the default temperature dependencies of the CO_2 compensation point in the absence of mitochondrial respiration (Γ^*) and the Michaelis–Menten constants for CO_2 and O_2 (K_c and K_o) taken from Bernacchi et al. (2001) study. Since the leaf mesophyll conductance for CO_2 was not measured, the reported V_{cmax} and J_{max} are *apparent* as they were parameterized based on intercellular CO_2 concentrations (C_i), rather than the CO_2 concentration at the site of carboxylation (C_c) in the chloroplast. The reported rates of V_{cmax} and J_{max} at their thermal optima ($V_{cmaxopt}$ and J_{maxopt}) were derived from the following modified Arrhenius function (Equation 4) outlined below (Medlyn et al., 2002):

$$f(T_k) = k_{opt}\frac{H_d \exp\left(\frac{E_a(T_k - T_{opt})}{T_k R T_{opt}}\right)}{H_d - E_a\left(1 - \exp\left(\frac{H_d(T_k - T_{opt})}{T_k R T_{opt}}\right)\right)}, \quad (4)$$

where k_{opt} is the process rate (e.g., V_{cmax} or J_{max}; μmol m^{-2} s^{-1}) at its optimal temperature ($V_{cmaxopt}$, and J_{maxopt}); H_d (kJ mol^{-1}) represents the deactivation energy term, which characterizes the reduction in enzyme activity as temperatures rise; E_a (kJ mol^{-1}) stands for the activation energy term, describing the exponential increase in enzyme activity with temperature elevation; R denotes the universal gas constant (8.314 J mol^{-1} K^{-1}), while T_{opt} and T_k correspond to the optimal and specified temperatures of the process rate (e.g., V_{cmax} or J_{max}; μmol m^{-2} s^{-1}). As it is commonly done in other studies, the value of H_d was fixed at 200 kJ mol^{-1} in order to avoid over-parameterization of Equation (4) (Dreyer et al., 2001; Medlyn et al., 2002). We used Equation (4) to also parameterize rates of V_{cmax} and J_{max} at prevailing mean growth temperature between 9 AM and 3 PM, when plants are most photosynthetically active. Mean growth temperature was defined as the average daytime air temperature over the 10 days preceding each tree measurement, based on previous studies that have demonstrated that photosynthesis acclimates within a 10-day period (Gunderson et al., 2010; Sendall et al., 2015; Smith & Dukes, 2017).

2.4 | Statistical analyses

To evaluate the effects of temperature and elevated CO_2 on photosynthetic capacity (V_{cmax} and J_{max}) and their ratios at various conditions—including the reference temperature of 25°C (V_{cmax25}, J_{max25} and J_{max25}/V_{cmax25}), the thermal optimum of each process ($V_{cmaxopt}$ and J_{maxopt}), and the mean growth temperature (V_{cmaxg} and J_{maxg})—as well as leaf nitrogen and leaf mass per unit area (LMA), we started with a linear mixed-effect model. In this model, warming and elevated CO_2 treatments, along with species, were designated as fixed effects, while the month during which the campaign was conducted was designated as the random effect. All analyses were run on the plot means with $n = 1$–4 trees/plot. The process of choosing the ultimate statistical model occurred in two stages, following the methodology outlined by Zuur et al. (2009). We first evaluated whether a random factor was required by comparing the model with the random intercept (i.e., month) and the one without any random structure. For this first step, we used the *gls* function in the model without the random structure and the *lme* function with the "Restricted maximum likelihood—REML" method in the model with the random structure, and both *gls* and *lme* functions are from the *nlme R* package (Pinheiro et al., 2023). We excluded the model featuring both random slope and intercept structures from the comparison, as our preliminary analyses suggested that it was over-parameterized. Thereafter, the model with the adequate random structure was selected based on the lowest akaike information criterion (AICc) (Supporting Information S1: Tables S1 and S2). When the model with random structure was not significantly different from the model without the random structure, we proceeded the analyses with a simple linear regression model. Following the determination of an appropriate random structure, we proceeded to choose the appropriate fixed effect structure. This involved considering both the model with only the main effects (i.e., warming, elevated CO_2, and species) without interactions and models incorporating all possible combinations of main effects and their interactions. The latter selection was done by comparing models with different structures using the "maximum likelihood—ML" method within the *gls* function from the *nlme R* package (Pinheiro et al., 2023). Similarly, the best fixed effect structure was selected based on the lowest AICc value using AICcmodavg R

package (Mazerolle, 2023) (Supporting Information S1: Tables S1 and S2). Last, three-way repeated measures ANOVA tests were used to analyse the main effects of growth temperature, growth CO_2, leaf temperature and their interactions on the responses of V_{cmax}, and J_{max} for each species using the *lmerTest* package (Kuznetsova et al., 2017). The random structure of this three-way repeated measures ANOVA involved leaf temperature nested within each measured tree, which was in turn nested within each experimental plot, and further nested within each month. To derive *p* value and respective statistical significance for each factor and interactions, we used the Type II Wald *F* tests with Kenward–Roger degrees of freedom (DF). All analyses were conducted in *R* (R Core Team, 2024).

3 | RESULTS

Except for the ratio of J_{max} to V_{cmax} at the thermal optimum and growth temperature, there were no significant differences across the two field campaigns (June and August 2017) on other measured leaf traits. Therefore, results of all other traits were lumped across June and August months. For all the studied photosynthetic traits, we did not find any interactive effects of warming and elevated CO_2 on their responses to these environmental factors, therefore, results below are reported for warming and elevated CO_2 separately.

3.1 | Temperature responses

The temperature response of V_{cmax} was significantly affected by warming in both species (Supporting Information S1: Figures S2, S3; Table S4). Furthermore, V_{cmax} was affected by warming differently when estimated at different reference temperatures. At a standard temperature of 25°C (V_{cmax25}), V_{cmax25} was not affected by warming in both species (Figure 1a,b; Supporting Information S1: Table S3). By contrast, V_{cmax} estimated at both the thermal optimum ($V_{cmaxopt}$; Figure 2a,b) and at growth temperature (V_{cmaxg}; Figure 3a,b), significantly increased with warming in both species (Supporting Information S1: Table S3). Across species, $V_{cmaxopt}$ increased by 3.3 $\mu mol\, m^{-2}\, s^{-1}$ per 1°C warming (Supporting Information S1: Table S3), while V_{cmaxg} increased by 3.65 $\mu mol\, m^{-2}\, s^{-1}$ per 1°C warming (Supporting Information S1: Table S3).

By contrast, the temperature response of J_{max} was largely not affected by growth temperature in both species (Supporting Information S1: Figures S4, S5; Table S4). However, similar to V_{cmax}, J_{max} also responded differently when estimated at different reference temperatures. J_{max} at 25°C, J_{max25}, was not affected by warming in both species (Figure 1c,d; Supporting Information S1: Table S3). Across the two species, J_{max} at the thermal optimum, J_{maxopt}, increased by 2.2 $\mu mol\, m^{-2}\, s^{-1}$ per 1°C warming (Figure 2c,d; Supporting Information S1: Table S3), while J_{max} at the prevailing growth temperature, J_{maxg}, marginally ($p = 0.064$) increased by 2 $\mu mol\, m^{-2}\, s^{-1}$ per 1°C warming (Figure 3c,d; Supporting Information S1: Table S3).

The ratio of J_{max} to V_{cmax} mirrored that of both V_{cmax} and J_{max}. At 25°C, warming did not affect this ratio (Figure 4; Supporting Information S1: Table S3). By contrast, the J_{max} to V_{cmax} ratio at both their thermal optima ($J_{maxopt}/V_{cmaxopt}$) and prevailing growth temperature (J_{maxg}/V_{cmaxg}) decreased with warming (Figure 4). Specifically, $J_{maxopt}/V_{cmaxopt}$ decreased by 0.025 per 1°C warming, while for the J_{maxg}/V_{cmaxg}, the slope was slightly steeper, decreasing on average by 0.032 per 1°C warming across the two species (Supporting Information S1: Table S3).

3.2 | Elevated CO_2 responses

The temperature response of both V_{cmax} and J_{max} was not significantly affected by elevated CO_2 in either species (Supporting Information S1: Figures S2–5; Table S4). Moreover, responses of both V_{cmax} and J_{max} estimated at any of the three reference temperatures (25°C, thermal optima and growth temperature) were consistent across the two species, as they were all significantly lower in plants grown under elevated CO_2 growth conditions compared to those grown under ambient CO_2 (Figures 1a,b; 2a,b; 3a,b; Supporting Information S1: Table S3). The V_{cmax25}, V_{cmaopt}, and V_{cmaxg} decreased by 28%, 36%, and 35%, respectively, in trees grown under elevated CO_2 compared to their ambient-CO_2 counterparts. For J_{max}, both J_{max25} and J_{maxopt} significantly decreased by 15% and 19%, respectively, while J_{maxg} decreased by 14%, but this decrease was not statistically significant, potentially driven by observed substantial variations in this trait ($p = 0.12$; Figures 1c,d; 2c,d; 3c,d; Supporting Information S1: Table S3). The ratio of J_{max25}/V_{cmax25}, $J_{maxopt}/V_{cmaxopt}$, and J_{maxg}/V_{cmaxg} increased by 16%, 18%, and 17%, respectively, in elevated CO_2-grown trees compared to those growing under ambient CO_2 conditions (Figure 5; Supporting Information S1: Table S3).

3.3 | Leaf nitrogen and leaf mass per unit area

Warming and elevated CO_2 treatments had similar effects on leaf nitrogen concentration on area basis (N_a) and leaf mass per leaf area (LMA) in both tamarack and black spruce (Figure 5; Supporting Information S1: Table S3). Leaf N_a was significantly impacted by warming and elevated CO_2 (without interaction) (Figure 5a,b; Supporting Information S1: Table S3). In response to warming, leaf N_a increased on average 0.043 $g\, m^{-2}$ per 1°C of warming across the two species. In response to elevated CO_2, leaf N_a was, on average, 20% lower in elevated CO_2-grown trees compared to those in ambient CO_2 conditions across the two species. By contrast, LMA was significantly affected by elevated CO_2 but not by warming across species (Figure 5c,d; Supporting Information S1: Table S3). Across the two species, LMA was, on

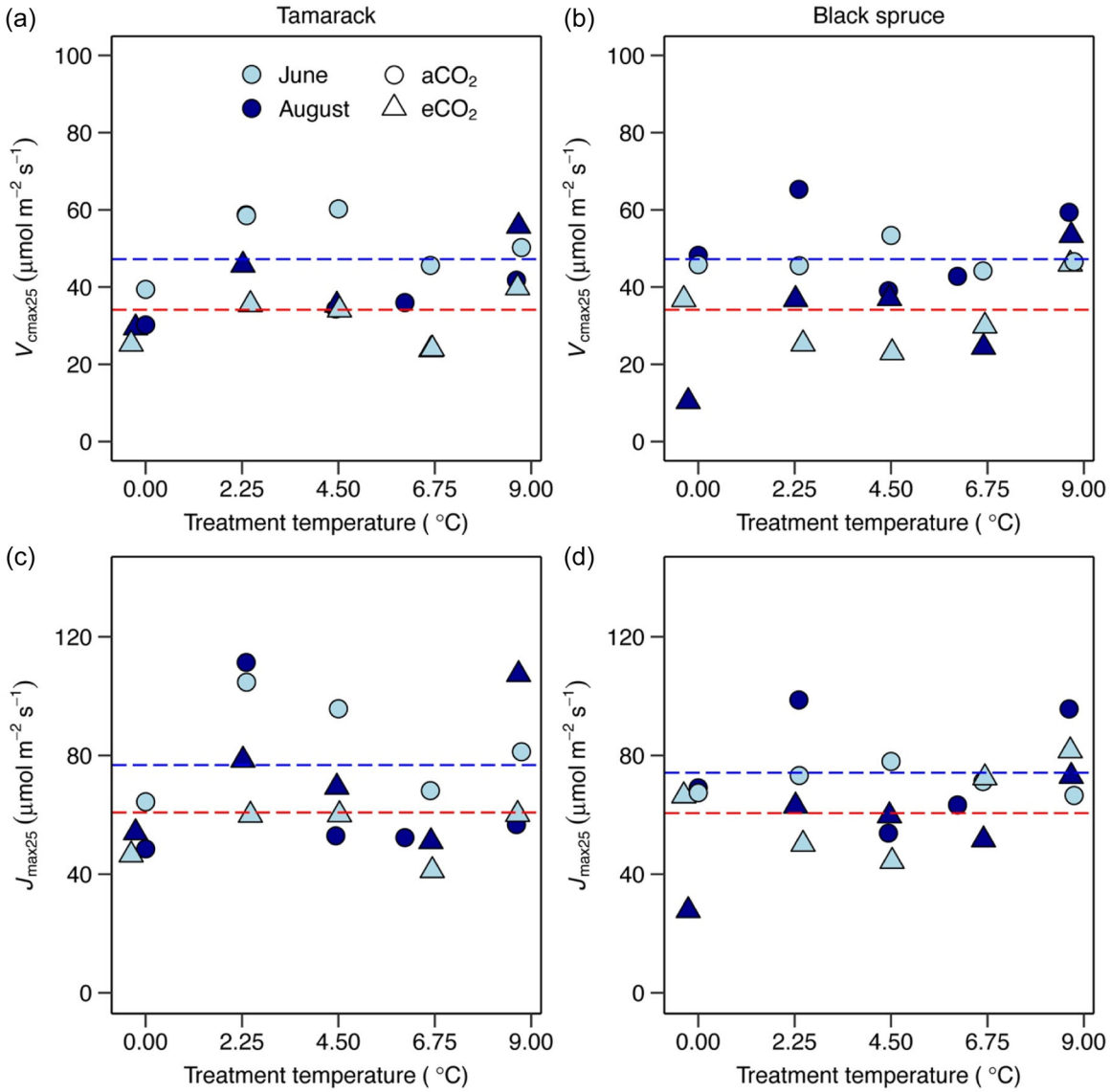

FIGURE 1 Impact of temperature and CO_2 treatments on photosynthetic capacity at a standard temperature of 25°C in tamarack (a, c) and black spruce (b, d). (a, b) The maximum carboxylation rate of Rubisco (V_{cmax25}; µmol m^{-2} s^{-1}) and (c, d) the maximum electron transport rate (J_{max25}; µmol m^{-2} s^{-1}). Symbol colours represent the month in which measurements were taken (June = light blue; August = dark blue). Symbol shapes represent CO_2 treatments (circle = ambient CO_2 – aCO_2; triangles = elevated CO_2 – eCO_2). Each data point represents the mean value of biologically independent trees measured in each plot (n = 1–4 trees/plot). Significance threshold: $p < 0.05$. Blue and red long-dashed lines represent regression lines at intercepts of aCO_2 and eCO_2, respectively, at slope of zero as there was no significant warming effect on the slope. Further details on statistical analyses for this figure can be found in Supporting Information S1: Table S3.

average, 18% higher in elevated CO_2 trees than in ambient CO_2 counterparts.

3.4 | Relationship between photosynthetic capacity and leaf nitrogen

Both V_{cmax25} and J_{max25} were positively related to leaf N_a in both species (Figure 6; Supporting Information S1: Table S4). To further explore whether leaf nitrogen have played a role in the response of photosynthetic capacity at a common leaf temperature of 25°C to the treatments, we normalised V_{cmax25} and J_{max25} to leaf N_a. In both species, both V_{cmax25}/N and J_{max25}/N did not significantly vary across warming treatments (Figure S6; Supporting Information S1: Table S3), suggesting that the lack of thermal acclimation of photosynthetic capacity could not largely be attributed to warming-induced effects on leaf N_a. By contrast, V_{cmax25}/N and J_{max25}/N were not significantly different between ambient and elevated CO_2-grown trees (Supporting Information S1: Table S3), suggesting that acclimation of both V_{cmax25} and J_{max25} to elevated strongly influenced changes in leaf N_a in elevated CO_2-grown trees.

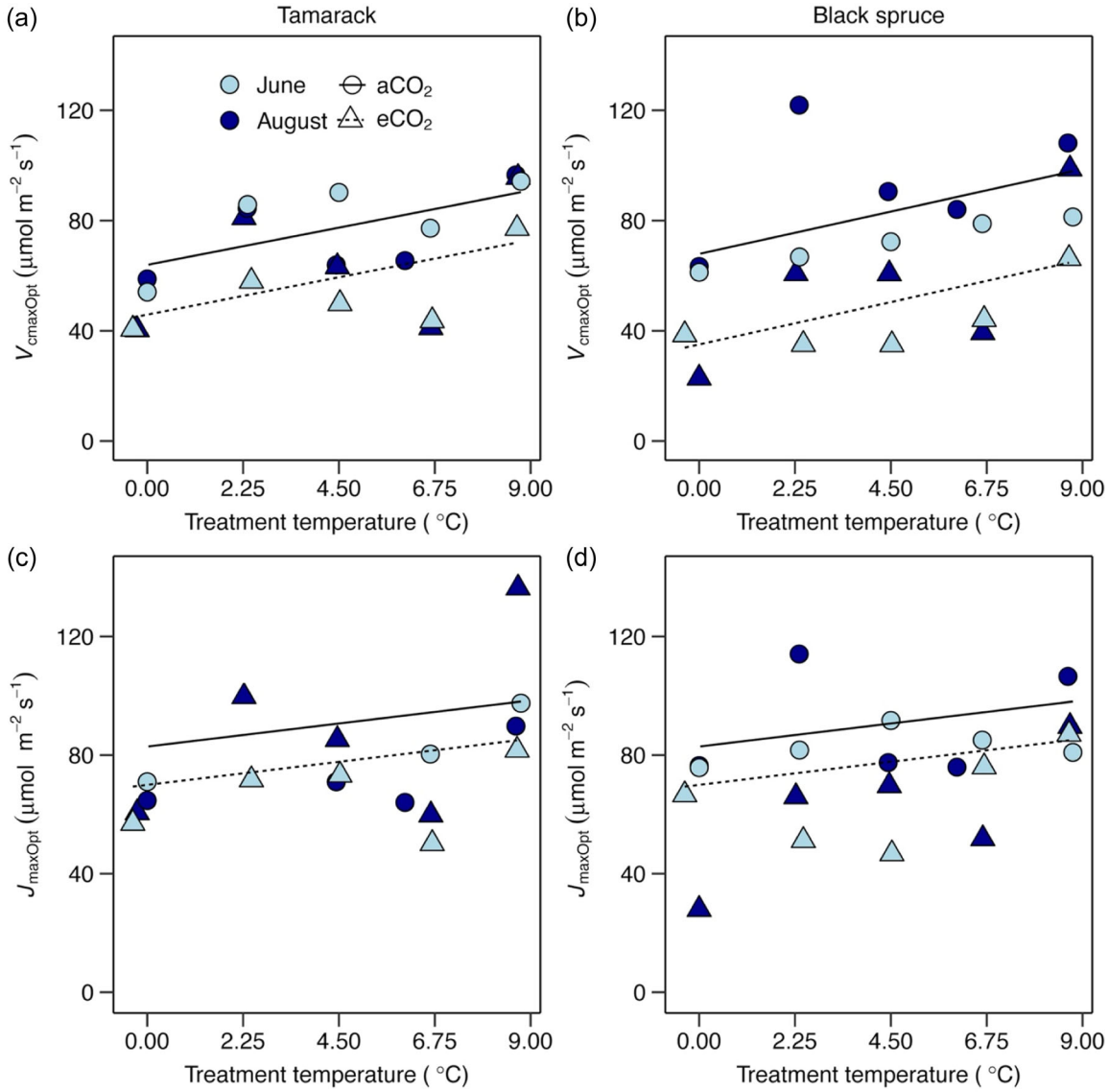

FIGURE 2 Impact of temperature and CO_2 treatments on photosynthetic capacity at its thermal optimum in tamarack (a, c) and black spruce (b, d). (a, b) The maximum carboxylation rate of Rubisco at the thermal optimum ($V_{cmaxOpt}$; µmol m^{-2} s^{-1}) and (c, d) the maximum electron transport rate at the thermal optimum (J_{maxOpt}; µmol m^{-2} s^{-1}). Symbol colours represent the month in which measurements were taken (June = light blue; August = dark blue). Symbol shapes represent CO_2 treatments (circle = ambient CO_2 – aCO_2; triangles = elevated CO_2 – eCO_2). Lines represent regression lines: the solid and the short-dashed lines represent ambient and elevated CO_2 treatments, respectively. Each data point represents the mean value of biologically independent trees measured in each plot (n = 1–4 trees/plot). Significance threshold: $p < 0.05$. Further details on statistical analyses for this figure can be found in Supporting Information S1: Table S3. [Color figure can be viewed at wileyonlinelibrary.com]

4 | DISCUSSION

In this study, we report findings from a field study that investigated the acclimation of photosynthetic capacity (V_{cmax} and J_{max}) to warming and elevated CO_2 after 2 years of a whole-ecosystem experimental warming (up to +9°C above ambient temperature) combined with 1 year of elevated CO_2 (+430–500 ppm above ambient atmospheric CO_2) in mature trees of North America's boreal conifers (black spruce and tamarack) at their southern range of natural distribution. We found that rates of V_{cmax} and J_{max} when measured at a common temperature of 25°C did not show any acclimation (i.e., did not change) to warming in either tamarack or black spruce (Figure 1). However, when measured at their thermal optima and prevailing growth temperature, both V_{cmax} and J_{max} increased with warming (i.e., acclimated) (Figures 2 and 3), suggesting that the ability to detect the thermal acclimation of photosynthetic capacity may partly depend on the chosen reference temperature. We also found that leaf N_a content, V_{cmax} and J_{max} all decreased in

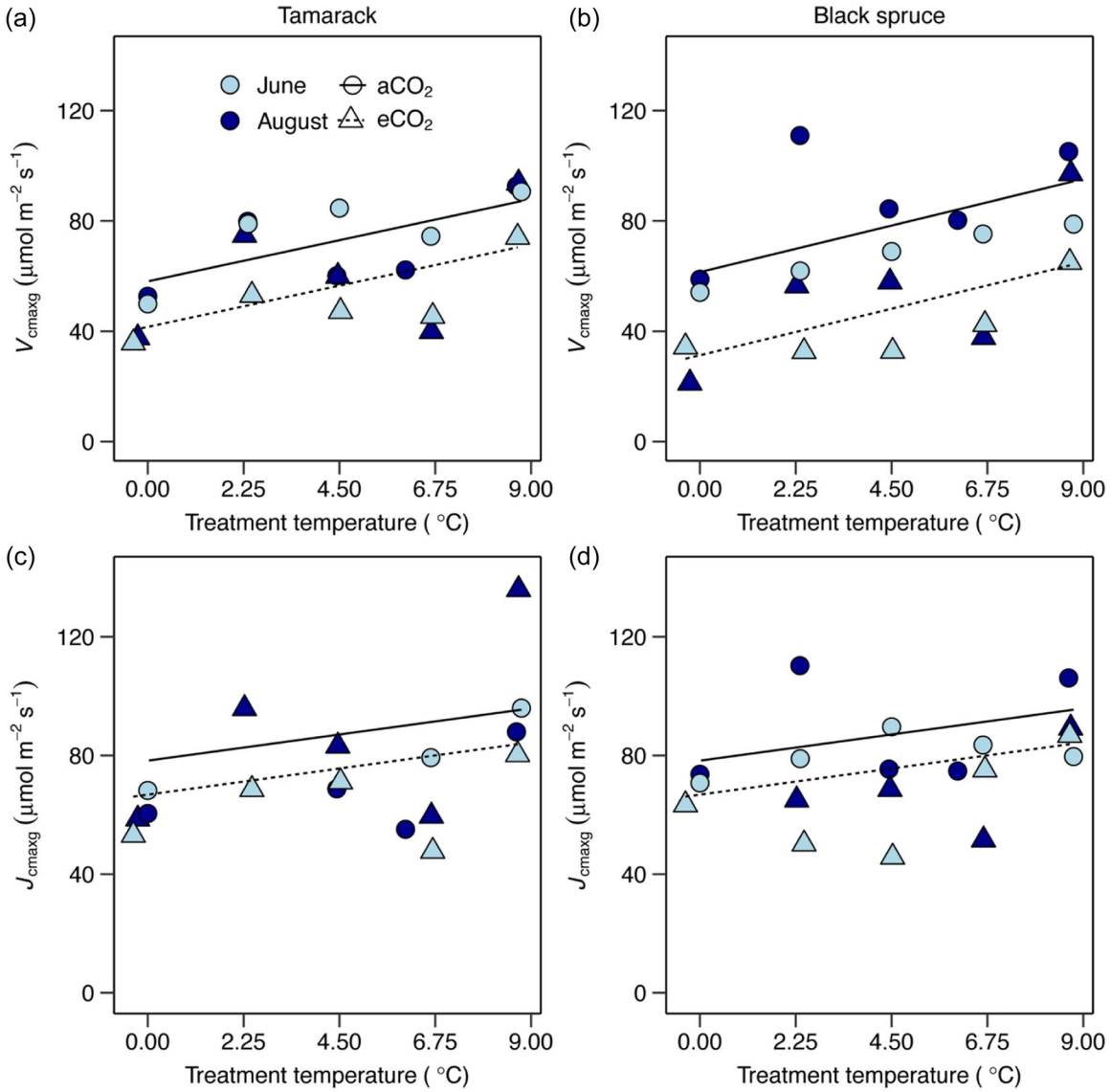

FIGURE 3 Impact of temperature and CO_2 treatments on photosynthetic capacity at prevailing growth temperature (9 AM–3 PM) in tamarack (a, c) and black spruce (b, d). (a, b) The maximum carboxylation rate of Rubisco at growth temperature (V_{cmaxg}; µmol m^{-2} s^{-1}) and (c, d) the maximum electron transport rate at growth temperature (J_{maxg}; µmol m^{-2} s^{-1}). Symbol colours represent the month in which measurements were taken (June = light blue; August = dark blue). Symbol shapes represent CO_2 treatments (circle = ambient CO_2 – aCO_2; triangles = elevated CO_2 – eCO_2). Lines represent regression lines: the solid and the short-dashed lines represent ambient and elevated CO_2 treatments, respectively. Each data point represents the mean value of biologically independent trees measured in each plot (n = 1–4 trees/plot). Significance threshold: $p < 0.05$. Further details on statistical analyses for this figure can be found in Supporting Information S1: Table S3. [Color figure can be viewed at wileyonlinelibrary.com]

concert to elevated CO_2 (i.e., acclimated) at any of the three reference temperature (Figures 1, 2, 3, 5; Supporting Information S1: Table S3). The J_{max}/V_{cmax} ratio decreased with warming (i.e., acclimated) at the thermal optima of the two processes and at prevailing growth temperature, but remained constant at 25°C. In response to elevated CO_2, J_{max}/V_{cmax} ratio increased with elevated CO_2 (i.e., acclimated) in both species and at the three reference temperatures (Figure 4). We did not find any interactive effect of warming and elevated CO_2 on any studied trait of photosynthetic capacity.

4.1 | Temperature responses of photosynthetic capacity

In both species, V_{cmax25} and J_{max25} did not significantly change with warming (Figure 1), partly rejecting our first hypothesis (H1), which proposed that both V_{cmax25} and J_{max25} should decrease with warming according to the least-optimality framework (Smith & Keenan, 2020; Wang et al., 2020). However, our results are in agreement with findings from meta-analyses (Crous et al., 2022; Kattge & Knorr, 2007; Kumarathunge et al., 2019; Way & Oren, 2010) and also those

Plant, Cell & Environment PC&E -WILEY

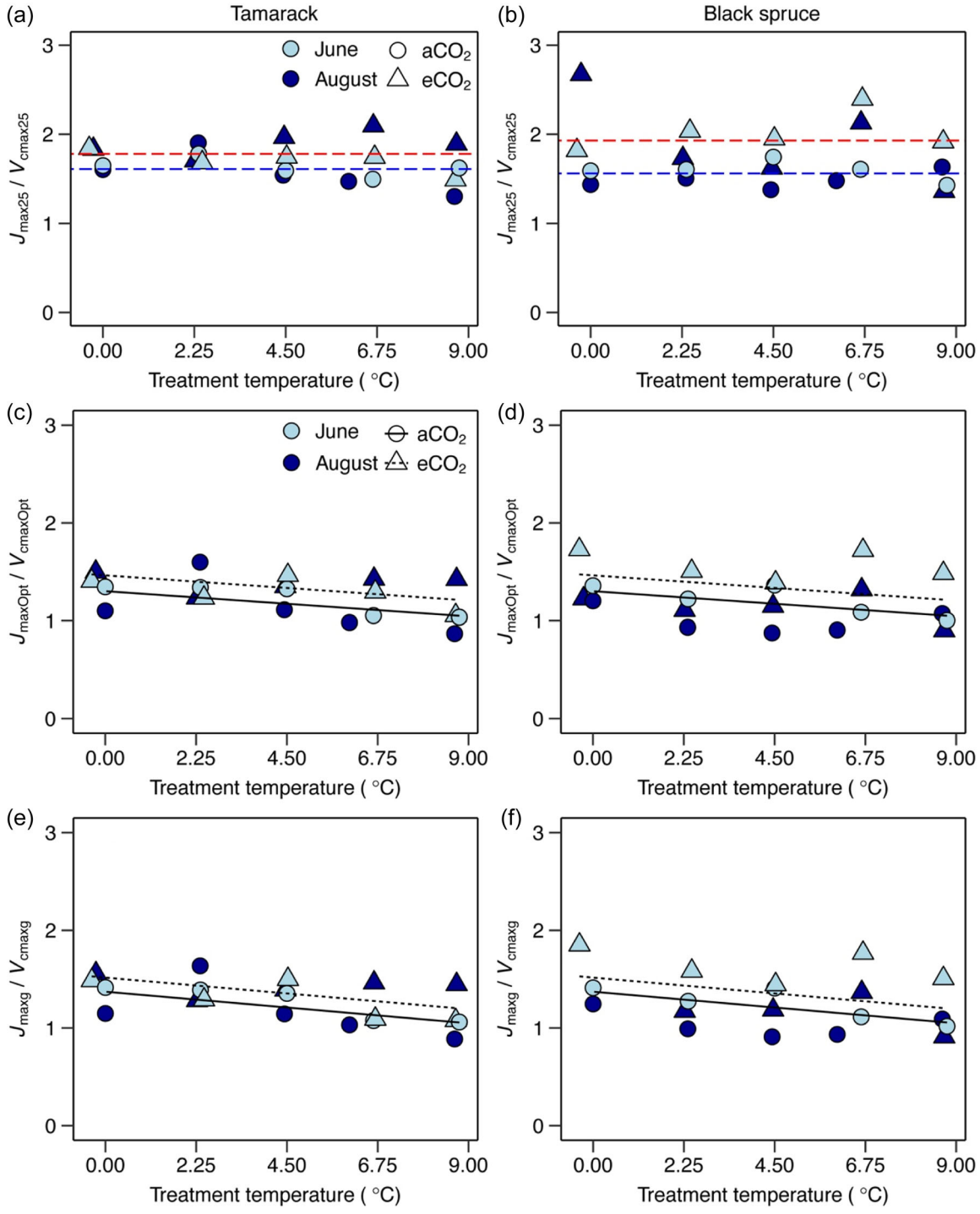

FIGURE 4 Impact of temperature and CO_2 treatments on the ratio of the maximum electron transport rate to the maximum carboxylation rate of Rubisco at photosynthetic capacity at a standard temperature of 25°C, at their thermal optima, and at prevailing growth temperature in tamarack (a, c) and black spruce (b, d). (a, b) The ratio of the maximum electron transport rate to the maximum carboxylation rate of Rubisco at (a, b) a standard temperature of 25°C (J_{max25}/V_{cmax25}), (c, d) at their thermal optima ($J_{maxOpt}/V_{cmaxOpt}$), and (e, f) at growth temperature (J_{maxg}/V_{cmaxg}). Symbol colours represent the month in which measurements were taken (June = light blue; August = dark blue). Symbol shapes represent CO_2 treatments (circle = ambient CO_2 – aCO_2; triangles = elevated CO_2 – eCO_2). In (a, b) blue and red long-dashed lines represent regression lines at intercepts of aCO_2 and eCO_2, respectively, at slope of zero as there was no significant warming effect on the slope. In (c–f) lines represent regression lines: the solid and the short-dashed lines represent ambient and elevated CO_2 treatments, respectively. Each data point represents the mean value of(n biologically independent trees measured in each plot (n = 1–4 trees/plot). Significance threshold: $p < 0.05$. Further details on statistical analyses for this figure can be found in Supporting Information S1: Table S3. [Color figure can be viewed at wileyonlinelibrary.com]

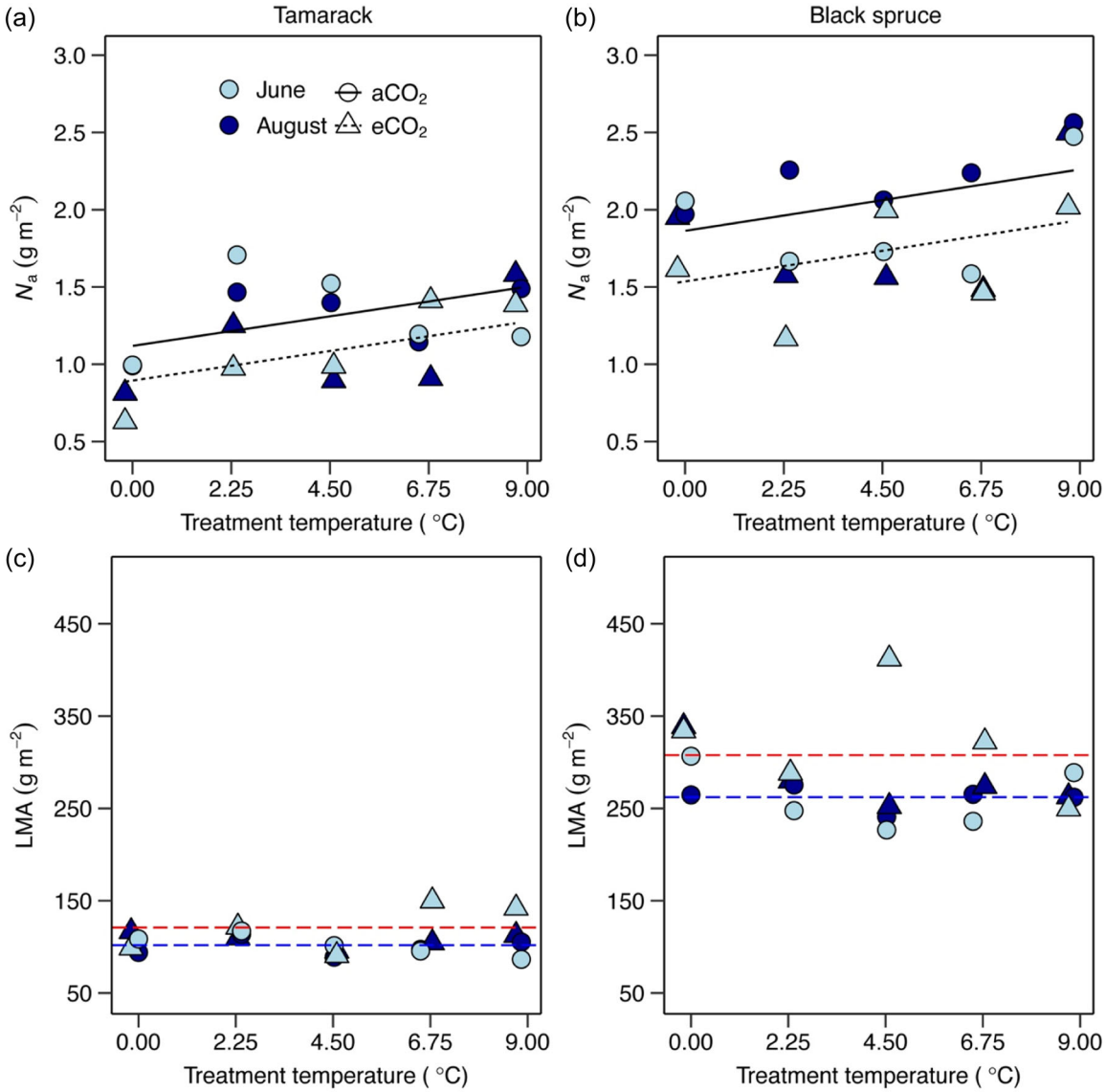

FIGURE 5 Impact of temperature and CO_2 treatments on (a, b) leaf nitrogen concentration per unit leaf area (N_a; g m^{-2}), and leaf mass per area in tamarack (a, c) and black spruce (b, d). Symbol colours represent the month in which measurements were taken (June = light blue; August = dark blue). Symbol shapes represent CO_2 treatments (circle = ambient CO_2 – aCO_2; triangles = elevated CO_2 – eCO_2). Lines represent regression lines: in (a, b) the solid and the short-dashed lines represent ambient and elevated CO_2 treatments, respectively. In (c, d) blue and red long-dashed lines represent regression lines at intercepts of aCO_2 and eCO_2, respectively, at slope of zero as there was no significant warming effect on the slope. Each data point represents the mean value of biologically independent trees measured in each plot (n = 1–4 trees/plot). Significance threshold: $p < 0.05$. Further details on statistical analyses for this figure can be found in Supporting Information S1: Table S3. [Color figure can be viewed at wileyonlinelibrary.com]

from recent experimental warming field studies on boreal and temperate seedlings (Bermudez et al., 2021; Stefanski et al., 2020), and European mature boreal conifers (Lamba et al., 2018). Nitrogen (N) is a key nutrient influencing variation of V_{cmax} and J_{max} rates (Ellsworth et al., 2022), and changes in leaf N were shown to be related to the thermal acclimation of V_{cmax} and J_{max} in some studies (Crous et al., 2018; Dusenge, Madhavji, et al., 2020, 2021; Scafaro et al., 2017; Way & Sage, 2008a). In our study, leaf N increased with warming, a response likely influenced by increases in soil nitrogen availability due to warming, as recently reported at our experimental site (Iversen et al., 2023). However, after normalizing V_{cmax25} and J_{max25} to leaf N (Supporting Information S1: Figure S6), photosynthetic capacity exhibited similar response to non-normalized values (i.e., no change), indicating that nitrogen have relatively little influence on thermal acclimation of these two processes. Recently, Stefanski et al. (2020) and Bermudez et al. (2021) suggested that the lack of thermal acclimation of V_{cmax25} and J_{max25} commonly observed in boreal experimental warming field studies may largely be due to modest warming treatments (~3 – 4°C above ambient) typically applied (Bermudez et al., 2021; Lamba et al., 2018; Smith et al., 2020;

Plant, Cell & Environment PC&E -WILEY

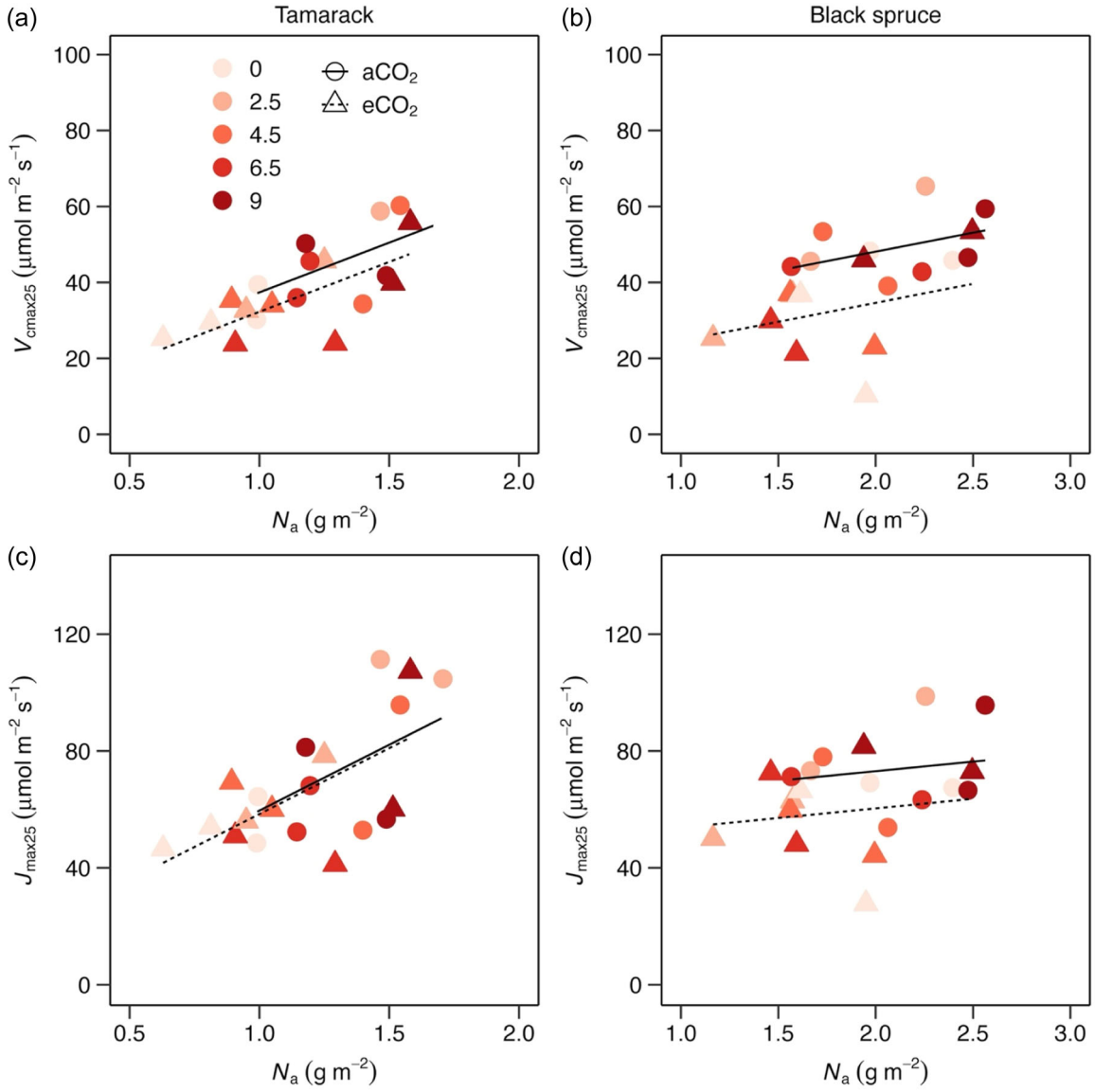

FIGURE 6 Relationship between photosynthetic capacity and leaf nitrogen for tamarack (a, c) and black spruce (b, d). (a, b) The maximum carboxylation rate of Rubisco (V_{cmax25}; µmol m^{-2} s^{-1}) and (c, d) the maximum electron transport rate (J_{max25}; µmol m^{-2} s^{-1}); leaf nitrogen concentration on area basis (N_a; g m^{-2}). Symbol shapes represent CO_2 treatments (circle = ambient CO_2 – aCO_2; triangles = elevated CO_2 – eCO_2). The red colour gradient represents different treatment temperatures with the lightest red representing ambient while darkest red represents the hottest (+9°C) treatment. Lines represent regression lines: the solid and the short-dashed lines represent ambient and elevated CO_2 treatments, respectively. Each data point represents the mean value of biologically independent trees measured in each plot (n = 1–4 trees/plot). Significance threshold: $p < 0.05$. Further details on statistical analyses for this figure can be found in Supporting Information S1: Table S4. [Color figure can be viewed at wileyonlinelibrary.com]

Stefanski et al., 2020). However, our study, which utilized incremental warming of 2.25°C up to 9°C—with the 9°C warming (and atmospheric CO_2 of >800 ppm) considered a likely scenario under the business as usual in some higher latitude regions by 2100 (IPCC, 2021), indicates that the lack of discernable acclimation of photosynthetic capacity to warming in realistic field conditions may be less dependent on the level of warming applied. Future studies that investigate warming effects on underlying photosynthetic biochemistry (e.g., Rubisco content and activation state, and photosynthetic pigments content) in field settings are still needed to fully understand the causes of this commonly observed lack of thermal acclimation of photosynthetic capacity at a given standard temperature, which also contradicts predictions of the least-cost optimality framework.

In contrast to photosynthetic capacity measured at 25°C, photosynthetic capacity measured at both the thermal optima of the respective process components ($V_{cmaxOpt}$ and J_{maxOpt}) and prevailing growth temperature increased with warming (Figures 2 and 3), suggesting a

positive acclimation response to warming in the studied species (Way & Yamori, 2014). These findings partly support H1, which proposed that both V_{cmaxg} and J_{maxg} should increase with warming according to the least-optimality framework (Smith et al., 2019; Smith & Keenan, 2020; Wang et al., 2020), and are consistent with results from previous studies (Scafaro et al., 2017; Smith & Dukes, 2017; Smith & Keenan, 2020; Way & Oren, 2010). This observed positive acclimation of photosynthetic capacity at the thermal optima and growth temperature suggests that V_{cmax} and J_{max} have acclimated to warming despite not being seen at the commonly used standard temperature of 25°C. In our companion SPRUCE study (Dusenge et al., 2023), we also found that the thermal optima of V_{cmax} and J_{max} in these species increased with warming, indicating a strong thermal acclimation of photosynthetic biochemistry in these boreal conifers. Overall, our findings indicate that the ability to detect the thermal acclimation of V_{cmax} and J_{max} depends on the chosen reference temperature and parameter of interest, since the shape of instantaneous temperature response of photosynthetic capacity and its acclimation response to increased growth temperature can be seen through several important temperature sensitivity parameters such as the activation energy (initial slope of the temperature response; E_{aVcmax} and E_{aJmax}), thermal optima ($T_{optVcmax}$ and $T_{optJmax}$), and deactivation energy (Kumarathunge et al., 2019; Way et al., 2014; Yamori et al., 2014) of these key processes.

The ratio of J_{max} to V_{cmax} (J_{max}/V_{cmax}) is another key parameter used for modelling photosynthesis within TBMs (Rogers, Medlyn, et al., 2017). At 25°C, J_{max}/V_{cmax} was constant across warming treatments, however, at both the thermal optima of the two processes and at prevailing growth temperature, J_{max}/V_{cmax} decreased with warming (i.e., acclimated) (Figure 4). Our results at 25°C, therefore, contradict findings from several studies (Bermudez et al., 2021; Dusenge et al., 2015, Dusenge, Madhavji, et al., 2020; Smith & McNellis, & Dukes, 2020; Stefanski et al., 2020) and meta-analysis (Crous et al., 2022; Kattge & Knorr, 2007; Kumarathunge et al., 2019) that commonly report a decrease in J_{max25}/V_{cmax25} to warming. However, a few other studies also did not observe a decrease of J_{max25}/V_{cmax25} with warming (Crous et al., 2018; Scafaro et al., 2017). Constant J_{max25}/V_{cmax25} in our study could largely be attributed to the observed lack of effect of warming on either V_{cmax25} or J_{max25}. However, responses at the thermal optimum and growth temperature are consistent with findings of previous studies (Murphy & Way, 2021; Smith & Dukes, 2017) and the least-cost optimality framework (Smith & Keenan, 2020). Decrease of the J_{max}/V_{cmax} with warming is proposed to be a mechanism that reduces photorespiration that simultaneously increases with rising growth temperature (Dusenge et al., 2019; Sage & Kubien, 2007) by allocating relatively more resources to Rubisco carboxylation (i.e., V_{cmax}) compared to the electron transport (i.e., J_{max}) process (Dusenge et al., 2021; Smith & Keenan, 2020).

4.2 | Elevated CO_2 responses of photosynthetic capacity

In our study, photosynthetic capacity generally acclimated to elevated CO_2, by decreasing in trees exposed to elevated CO_2 regardless of the reference temperature (Figures 1–3; Supporting Information S1: Table S3), and this response agrees with our second hypothesis (H2). Both V_{cmax} and J_{max} strongly acclimated to elevated CO_2, with V_{cmax} showing relatively stronger acclimation response to elevated CO_2 (−28% to −36%) compared to J_{max} (−14% to −19%). Observed reductions in V_{cmax} and J_{max} in our study are largely consistent with findings from meta-analyses, which are dominated by studies on temperate tree species and crops (Ainsworth & Long, 2005; Ainsworth & Rogers, 2007; Leakey et al., 2009; Smith & Keenan, 2020), but partly contrast predictions of the least-cost optimality theory which predicts rather slight positive responses of J_{max} to elevated CO_2 (Smith & Keenan, 2020). Consequently, the ratio of J_{max} to V_{cmax} at all three reference temperatures was higher (16%–17%; Figure 4, Supporting Information S1: Table S3) in trees exposed to elevated CO_2 compared to those growing in ambient atmospheric CO_2 conditions. The latter findings are consistent with results from a few previous studies conducted mainly on seedlings in highly controlled growth conditions (Crous et al., 2013; Dusenge, Madhavji, et al., 2020; Smith & Keenan, 2020). There has been relatively fewer studies on long-term CO_2 responses of photosynthetic capacity of mature boreal conifer trees in realistic field conditions. Before our study, we are aware of only one field study on mature trees of Norway spruce which showed that V_{cmax} strongly acclimated to elevated CO_2 (i.e., −23%), but the study did not investigate the responses of J_{max} (Lamba et al., 2018). Therefore, our current study, further generally adds results on long-term acclimation of J_{max} and J_{max}/V_{cmax} ratio to elevated CO_2 for the mature boreal conifers.

4.3 | Responses of photosynthetic capacity to combined warming and elevated CO_2

Our study did not find any interactive effect of temperature and elevated CO_2 on V_{cmax} and J_{max} at any reference temperature (Supporting Information S1: Table S3), supporting our third hypothesis (H3). Our findings also support the predictions of the least-cost optimality framework, where a strong interaction of warming and elevated CO_2 on rates of photosynthetic capacity is not expected, and that responses of photosynthetic capacity to combined warming and elevated CO_2 should be comparable to their independent effects (see Figure 4 in Smith & Keenan, 2020). Several previous studies also did not find any interactions of warming and elevated CO_2 on either V_{cmax}, J_{max}, instead showing that V_{cmax} and J_{max} at a standard temperature acclimate to: (1) warming but not elevated CO_2 (Crous et al., 2013; Dusenge et al. 2020; Ghannoum et al., 2010; Kellomaki and Wang, 1996); (2) elevated CO_2 but not warming (Fauset et al., 2019; Ghannoum et al., 2010; Lamba et al., 2018); or (3) neither of these two factors (Murphy & Way, 2021; Wang, 1996). Clearly, there is an urgent need for more studies that focus on unraveling the biochemical mechanisms underlying the responses of V_{cmax} and J_{max} to warming and elevated CO_2. Such studies are essential for improving our understanding of photosynthetic

responses and modelling under both warming and elevated CO_2 growth conditions.

In summary, our study showed that the photosynthetic capacity (V_{cmax} and J_{max}) of mature trees of North American boreal conifers responded independently to warming and elevated CO_2 when exposed to both environmental factors. Our results are consistent with several previous studies that predominantly focused on younger trees, suggesting that ontogeny minimally influences these parameters' responses to global change factors. Furthermore, our results add to growing empirical evidence that the representation of photosynthesis within TBMs under both warming and elevated CO_2 could incorporate their effects independently. However, our study was confined to two boreal conifer species. Therefore, we advocate for future research encompassing a broader spectrum of boreal species, diverse plant functional types, and other biomes to understand the widespread nature of the observed responses.

CODE AVAILABILITY

The R codes used for analyses for each figure included in this paper can be accessed at https://doi.org/10.6084/m9.figshare.23685984.v2.

ACKNOWLEDGEMENTS

Research was sponsored by the Biological and Environmental Research Program in the Office of Science, U.S. Department of Energy managed by UT- Battelle, LLC, for the U.S. Department of Energy under contract DEAC05-00OR22725. M.E.D., J.M.W., E.J.W., D.A.M., A.W.K. and P.J.H. were supported under this contract. E.J.W. also acknowledges support from USGS Climate Research and Development Program. P.B.R., A.S., R.B., and R.A.M acknowledge funding support by the U.S. NSF Biological Integration Institutes grant DBI-2021898. D.A.W. acknowledges funding from the NSERC Discovery and Strategic programs (RGPIN/04677-2019 and STPGP/521445-2018), the Research School of Biology at the Australian National University, and the U.S. Department of Energy contract No. DE-SC0012704 to Brookhaven National Laboratory. Notice: This manuscript has been authored by UT-Battelle, LLC, under contract DE-AC05-00OR22725 with the US Department of Energy (DOE). The US government retains and the publisher, by accepting the article for publication, acknowledges that the US government retains a nonexclusive, paid-up, irrevocable, worldwide license to publish or reproduce the published form of this manuscript, or allow others to do so, for US government purposes. DOE will provide public access to these results of federally sponsored research in accordance with the DOE Public Access Plan (http://energy.gov/downloads/doe-public-access-plan). The DOI link for the data set used in this paper can be accessed at https://doi.org/10.25581/spruce.056/1455138 (Dusenge, Ward, et al., 2020) and https://doi.org/10.6084/m9.figshare.23685984.v2. Any use of trade, firm, or product names is for descriptive purposes only and does not imply endorsement by the U.S. Government.

CONFLICT OF INTEREST STATEMENT

The authors declare no conflict of interest.

DATA AVAILABILITY STATEMENT

The data that support the findings of this study are openly available in Figshare at https://doi.org/10.6084/m9.figshare.23685984.v2. The raw and processed (i.e., mean values used to generate each figure in the paper) photosynthetic capacity data generated in this study have been deposited in the figshare database and can be accessed at https://doi.org/10.6084/m9.figshare.23685984.v2. The complete leaf gas exchange data, including the data used in this paper, are also available through the SPRUCE project website at https://doi.org/10.25581/spruce.056/1455138.

ORCID

Mirindi Eric Dusenge http://orcid.org/0000-0003-4218-0911
Jeffrey M. Warren http://orcid.org/0000-0002-0680-4697
Peter B. Reich http://orcid.org/0000-0003-4424-662X
Eric J. Ward http://orcid.org/0000-0002-5047-5464
Bridget K. Murphy http://orcid.org/0000-0002-3574-6764
Artur Stefanski http://orcid.org/0000-0002-5412-1014
Marisol Cruz http://orcid.org/0000-0002-3015-8568
David A. McLennan http://orcid.org/0000-0002-1874-2614
Paul J. Hanson http://orcid.org/0000-0001-7293-3561
Danielle A. Way http://orcid.org/0000-0003-4801-5319

REFERENCES

Ainsworth, E.A. & Long, S.P. (2005) What have we learned from 15 years of free-air CO_2 enrichment (FACE)? A meta-analytic review of the responses of photosynthesis, canopy properties and plant production to rising CO_2. *New Phytologist*, 165, 351–372.

Ainsworth, E.A. & Rogers, A. (2007) The response of photosynthesis and stomatal conductance to rising [CO2]: mechanisms and environmental interactions. *Plant, Cell & Environment*, 30, 258–270.

Akalusi, M.E., Meng, F.R. & P.-A. Bourque, C. (2021) Photosynthetic parameters and stomatal conductance in attached and detached balsam fir foliage. *Plant-Environment Interactions*, 2, 206–215.

Beer, C., Reichstein, M., Tomelleri, E., Ciais, P., Jung, M., Carvalhais, N. et al. (2010) Terrestrial gross carbon dioxide uptake: global distribution and covariation with climate. *Science*, 329, 834–838.

Bermudez, R., Stefanski, A., Montgomery, R.A. & Reich, P.B. (2021) Short- and long-term responses of photosynthetic capacity to temperature in four boreal tree species in a free-air warming and rainfall manipulation experiment. *Tree Physiology*, 41(1), 89–102. Available from: https://doi.org/10.1093/treephys/tpaa115

Bernacchi, C.J., Singsaas, E.L., Pimentel, C., Portis Jr., A.R. & Long, S.P. (2001) Improved temperature response functions for models of rubisco-limited photosynthesis. *Plant, Cell & Environment*, 24, 253–259.

Bigras, F.J. & Bertrand, A. (2006) Responses of *Picea mariana* to elevated CO_2 concentration during growth, cold hardening and dehardening: phenology, cold tolerance, photosynthesis and growth. *Tree Physiology*, 26, 875–888.

von Caemmerer, S. (2000) *Biochemical models of leaf photosynthesis*. CSIRO Publishing.

Crous, K.Y., Drake, J.E., Aspinwall, M.J., Sharwood, R.E., Tjoelker, M.G. & Ghannoum, O. (2018) Photosynthetic capacity and leaf nitrogen decline along a controlled climate gradient in provenances of two widely distributed eucalyptus species. *Global Change Biology*, 24, 4626–4644.

Crous, K.Y., Quentin, A.G., Lin, Y.-S., Medlyn, B.E., Williams, D.G., Barton, C.V.M. et al. (2013) Photosynthesis of temperate *eucalyptus globulus* trees outside their native range has limited adjustment to

elevated CO_2 and climate warming. *Global Change Biology*, 19, 3790–3807.

Crous, K.Y., Uddling, J. & De Kauwe, M.G. (2022) Temperature responses of photosynthesis and respiration in evergreen trees from boreal to tropical latitudes. *New Phytologist*, 234, 353–374.

Dang, Q.-L., Margolis, H.A., Coyea, M.R., Sy, M. & Collatz, G.J. (1997) Regulation of branch-level gas exchange of boreal trees: roles of shoot water potential and vapor pressure difference. *Tree Physiology*, 17, 521–535.

Dreyer, E., Le Roux, X., Montpied, P., Daudet, F.A. & Masson, F. (2001) Temperature response of leaf photosynthetic capacity in seedlings from seven temperate tree species. *Tree Physiology*, 21, 223–232.

Dusenge, M., Ward, E.J., Warren, J.M., McLennan, D.A., Stinziano, J.R. & Murphy, B.K. et al. (2020) SPRUCE photosynthesis and respiration of *Picea mariana* and *Larix laricina* in SPRUCE experimental plots, 2016–2017. Oak Ridge National Laboratory (ORNL), Oak Ridge, TN (United States).

Dusenge, M.E., Duarte, A.G. & Way, D.A. (2019) Plant carbon metabolism and climate change: elevated CO2 and temperature impacts on photosynthesis, photorespiration and respiration. *New Phytologist*, 221, 32–49.

Dusenge, M.E., Madhavji, S. & Way, D.A. (2020) Contrasting acclimation responses to elevated CO_2 and warming between an evergreen and a deciduous boreal conifer. *Global Change Biology*, 26, 3639–3657.

Dusenge, M.E., Wallin, G., Gårdesten, J., Niyonzima, F., Adolfsson, L., Nsabimana, D. et al. (2015) Photosynthetic capacity of tropical montane tree species in relation to leaf nutrients, successional strategy and growth temperature. *Oecologia*, 177, 1183–1194.

Dusenge, M.E., Warren, J.M., Reich, P.B., Ward, E.J., Murphy, B.K., Stefanski, A. et al. (2023) Boreal conifers maintain carbon uptake with warming despite failure to track optimal temperatures. *Nature Communications*, 14, 4667.

Dusenge, M.E., Wittemann, M., Mujawamariya, M., Ntawuhiganayo, E.B., Zibera, E., Ntirugulirwa, B. et al. (2021) Limited thermal acclimation of photosynthesis in tropical montane tree species. *Global Change Biology*, 27, 4860–4878.

Duursma, R.A. (2015) Plantecophys—An R package for analysing and modelling leaf gas exchange data. *PLoS One*, 10, e0143346.

Ellsworth, D.S., Crous, K.Y., De Kauwe, M.G., Verryckt, L.T., Goll, D., Zaehle, S. et al. (2022) Convergence in phosphorus constraints to photosynthesis in forests around the world. *Nature Communications*, 13, 5005.

Farquhar, G.D., von Caemmerer, S. & Berry, J.A. (1980) A biochemical model of photosynthetic CO_2 assimilation in leaves of C 3 species. *Planta*, 149, 78–90.

Fauset, S., Oliveira, L., Buckeridge, M.S., Foyer, C.H., Galbraith, D., Tiwari, R. et al. (2019) Contrasting responses of stomatal conductance and photosynthetic capacity to warming and elevated CO2 in the tropical tree species *Alchornea glandulosa* under heatwave conditions. *Environmental and Experimental Botany*, 158, 28–39.

Garen, J.C., Branch, H.A., Borrego, I., Blonder, B., Stinziano, J.R. & Michaletz, S.T. (2022) Gas exchange analysers exhibit large measurement error driven by internal thermal gradients. *New Phytologist*, 236, 369–384.

Ghannoum, O., Phillips, N.G., Sears, M.A., Logan, B.A., Lewis, J.D., Conroy, J.P. et al. (2010) Photosynthetic responses of two eucalypts to industrial-age changes in atmospheric [CO2] and temperature. *Plant, Cell & Environment*, 33, 1671–1681.

Gunderson, C.A., O'Hara, K.H., Campion, C.M., Walker, A.V. & Edwards, N.T. (2010) Thermal plasticity of photosynthesis: the role of acclimation in forest responses to a warming climate. *Global Change Biology*, 16, 2272–2286.

Hanson, P.J., Riggs, J.S., Nettles, W.R., Phillips, J.R., Krassovski, M.B., Hook, L.A. et al. (2017) Attaining whole-ecosystem warming using air and deep-soil heating methods with an elevated CO_2 atmosphere. *Biogeosciences*, 14, 861–883.

Houghton, R.A. (2007) Balancing the global carbon budget. *Annual Review of Earth and Planetary Sciences*, 35, 313–347.

IPCC. (2013) Contribution of working group I to the fifth assessment report of the intergovernmental panel on climate change. In: Stocker, T.F., Qin, D., Plattner, G.K., Tignor, M., Allen, S.K., Boschung, J., Nauels, A., Xia, Y., Bex, V. & Midgley, P.M. (Eds.) *Climate change 2013 the physical science basis*. Cambridge, United Kingdom: Cambridge University Press, pp. 1535.

IPCC. (2021) Contribution of working group I to the sixth assessment report of the intergovernmental panel on climate change. In: Masson-Delmotte, V., Zhai, P., Pirani, A., Connors, S.L., Péan, C., Berger, S., Caud, N., Chen, Y., Goldfarb, L., Gomis, M.I., Huang, M., Leitzell, K., Lonnoy, E., Matthews, J.B.R., Maycock, T.K., Waterfield, T., Yelekçi, O., Yu, R. & Zhou, B. (Eds.) *Climate change 2021 the physical science basis*. Cambridge, United Kingdom: Cambridge University Press, pp. 2391.

Iversen, C.M., Latimer, J., Brice, D.J., Childs, J., Vander Stel, H.M., Defrenne, C.E. et al. (2023) Whole-Ecosystem warming increases plant-available nitrogen and phosphorus in an ombrotrophic bog. *Ecosystems*, 26(1), 86–113. Available from: https://doi.org/10.1007/s10021-022-00744-x

Jiang, C., Ryu, Y., Wang, H. & Keenan, T.F. (2020) An optimality-based model explains seasonal variation in C3 plant photosynthetic capacity. *Global Change Biology*, 26, 6493–6510.

Kattge, J. & Knorr, W. (2007) Temperature acclimation in a biochemical model of photosynthesis: a reanalysis of data from 36 species. *Plant, Cell & Environment*, 30, 1176–1190.

Kellomaki, S. & Wang, K.Y. (1996) Photosynthetic responses to needle water potentials in Scots pine after a four-year exposure to elevated CO2 and temperature. *Tree Physiology*, 16, 765–772.

Knauer, J., Cuntz, M., Smith, B., Canadell, J.G., Medlyn, B.E., Bennett, A.C. et al. (2023) Higher global gross primary productivity under future climate with more advanced representations of photosynthesis. *Science Advances*, 9, eadh9444.

Kumarathunge, D.P., Medlyn, B.E., Drake, J.E., Tjoelker, M.G., Aspinwall, M.J., Battaglia, M. et al. (2019) Acclimation and adaptation components of the temperature dependence of plant photosynthesis at the global scale. *New Phytologist*, 222, 768–784.

Kuznetsova, A., Brockhoff, P.B. & Christensen, R.H.B. (2017) lmerTest package: tests in linear mixed effects models. *Journal of Statistical Software*, 82(13), 1–26. Available from: https://doi.org/10.18637/jss.v082.i13

Lamba, S., Hall, M., Räntfors, M., Chaudhary, N., Linder, S., Way, D. et al. (2018) Physiological acclimation dampens initial effects of elevated temperature and atmospheric CO2 concentration in mature boreal Norway spruce. *Plant, Cell & Environment*, 41, 300–313.

Leakey, A.D.B., Ainsworth, E.A., Bernacchi, C.J., Rogers, A., Long, S.P. & Ort, D.R. (2009) Elevated CO2 effects on plant carbon, nitrogen, and water relations: six important lessons from FACE. *Journal of Experimental Botany*, 60, 2859–2876.

Lombardozzi, D.L., Bonan, G.B., Smith, N.G., Dukes, J.S. & Fisher, R.A. (2015) Temperature acclimation of photosynthesis and respiration: A key uncertainty in the carbon cycle-climate feedback. *Geophysical Research Letters*, 42, 8624–8631.

Lu, X., Ju, W., Li, J., Croft, H., Chen, J.M., Luo, Y. et al. (2020) Maximum carboxylation rate estimation with chlorophyll content as a proxy of rubisco content. *Journal of Geophysical Research: Biogeosciences*, 125(8), e2020JG005748.

Maire, V., Martre, P., Kattge, J., Gastal, F., Esser, G., Fontaine, S. et al. (2012) The coordination of leaf photosynthesis links C and N fluxes in C3 plant species. *PLoS One*, 7, e38345.

Mazerolle, M.J. (2023). _AICcmodavg: Model selection and multimodel inference based on (Q)AIC(c)_. R package version 2.3.3, https://cran.r-project.org/package=AICcmodavg

Medlyn, B.E., Dreyer, E., Ellsworth, D., Forstreuter, M., Harley, P.C., Kirschbaum, M.U.F. et al. (2002) Temperature response of parameters of a biochemically based model of photosynthesis. II. A review of experimental data. *Plant, Cell & Environment*, 25, 1167–1179.

Mercado, L.M., Medlyn, B.E., Huntingford, C., Oliver, R.J., Clark, D.B., Sitch, S. et al. (2018) Large sensitivity in land carbon storage due to geographical and temporal variation in the thermal response of photosynthetic capacity. *New Phytologist*, 218, 1462–1477.

Murphy, B.K. & Way, D.A. (2021) Warming and elevated CO2 alter tamarack C fluxes, growth and mortality: evidence for heat stress-related C starvation in the absence of water stress. *Tree Physiology*, 41, 2341–2358.

Norby, R.J. & Luo, Y. (2004) Evaluating ecosystem responses to rising atmospheric CO_2 and global warming in a multi-factor world. *New Phytologist*, 162, 281–293.

Ofori-Amanfo, K.K., Klem, K., Veselá, B., Holub, P., Agyei, T., Marek, M.V. et al. (2020) Interactive effect of elevated CO_2 and reduced summer precipitation on photosynthesis is species-specific: the case study with soil-planted Norway Spruce and Sessile Oak in a mountainous forest plot. *Forests*, 12, 42.

Oliver, R.J., Mercado, L.M., Clark, D.B., Huntingford, C., Taylor, C.M., Vidale, P.L. et al. (2022) Improved representation of plant physiology in the JULES-vn5.6 land surface model: Photosynthesis, stomatal conductance and thermal acclimation.

Pinheiro, J. & Bates, D., & R Core Team (2023). _nlme: Linear and Nonlinear Mixed Effects Models_. R package version 3.1–164, https://CRAN.R-project.org/package=nlme

Prentice, I.C., Dong, N., Gleason, S.M., Maire, V. & Wright, I.J. (2014) Balancing the costs of carbon gain and water transport: testing a new theoretical framework for plant functional ecology. *Ecology Letters*, 17, 82–91.

R Core Team (2024). _R: a language and environment for statistical computing_. Vienna, Austria: R Foundation for Statistical Computing. https://www.R-project.org/

Rogers, A. (2014) The use and misuse of V(c,max) in earth system models. *Photosynthesis Research*, 119, 15–29.

Rogers, A., Medlyn, B.E., Dukes, J.S., Bonan, G., von Caemmerer, S., Dietze, M.C. et al. (2017) A roadmap for improving the representation of photosynthesis in Earth system models. *The New Phytologist*, 213, 22–42.

Rogers, A., Serbin, S.P., Ely, K.S., Sloan, V.L. & Wullschleger, S.D. (2017) Terrestrial biosphere models underestimate photosynthetic capacity and CO_2 assimilation in the Arctic. *The New Phytologist*, 216, 1090–1103.

Rogers, A., Serbin, S.P. & Way, D.A. (2022) Reducing model uncertainty of climate change impacts on high latitude carbon assimilation. *Global Change Biology*, 28, 1222–1247.

Sage, R.F. & Kubien, D.S. (2007) The temperature response of C(3) and C (4) photosynthesis. *Plant, Cell & Environment*, 30, 1086–1106.

Scafaro, A.P., Xiang, S., Long, B.M., Bahar, N.H.A., Weerasinghe, L.K., Creek, D. et al. (2017) Strong thermal acclimation of photosynthesis in tropical and temperate wet-forest tree species: the importance of altered rubisco content. *Global Change Biology*, 23, 2783–2800.

Sendall, K.M., Reich, P.B., Zhao, C., Jihua, H., Wei, X., Stefanski, A. et al. (2015) Acclimation of photosynthetic temperature optima of temperate and boreal tree species in response to experimental forest warming. *Global Change Biology*, 21, 1342–1357.

Slot, M., Rifai, S.W. & Winter, K. (2021) Photosynthetic plasticity of a tropical tree species, *tabebuia rosea*, in response to elevated temperature and [CO2]. *Plant, Cell & Environment*, 44, 2347–2364.

Smith, N.G. & Dukes, J.S. (2013) Plant respiration and photosynthesis in global-scale models: incorporating acclimation to temperature and CO2. *Global Change Biology*, 19, 45–63.

Smith, N.G. & Dukes, J.S. (2017) Short-term acclimation to warmer temperatures accelerates leaf carbon exchange processes across plant types. *Global Change Biology*, 23, 4840–4853.

Smith, N.G. & Keenan, T.F. (2020) Mechanisms underlying leaf photosynthetic acclimation to warming and elevated CO2 as inferred from least-cost optimality theory. *Global Change Biology*, 26, 5202–5216.

Smith, N.G., Keenan, T.F., Colin Prentice, I., Wang, H., Wright, I.J., Niinemets, Ü. et al. (2019) Global photosynthetic capacity is optimized to the environment. *Ecology Letters*, 22, 506–517.

Smith, N.G., McNellis, R. & Dukes, J.S. (2020) No acclimation: instantaneous responses to temperature maintain homeostatic photosynthetic rates under experimental warming across a precipitation gradient in *Ulmus americana*. *AoB Plants*, 12, plaa027.

Stefanski, A., Bermudez, R., Sendall, K.M., Montgomery, R.A. & Reich, P.B. (2020) Surprising lack of sensitivity of biochemical limitation of photosynthesis of nine tree species to open-air experimental warming and reduced rainfall in a Southern boreal forest. *Global Change Biology*, 26(2), 746–759. Available from: https://doi.org/10.1111/gcb.14805

Stinziano, J.R., Bauerle, W.L. & Way, D.A. (2019) Modelled net carbon gain responses to climate change in boreal trees: impacts of photosynthetic parameter selection and acclimation. *Global Change Biology*, 25, 1445–1465.

Wang, H., Atkin, O.K., Keenan, T.F., Smith, N.G., Wright, I.J., Bloomfield, K.J. et al. (2020) Acclimation of leaf respiration consistent with optimal photosynthetic capacity. *Global Change Biology*, 26, 2573–2583.

Wang, K. (1996) Acclimation of photosynthetic parameters in Scots pine after three years exposure to elevated temperature and CO2. *Agricultural and Forest Meteorology*, 82, 195–217.

Wang, L., Zheng, J., Wang, G. & Dang, Q.-L. (2022) Increased leaf area compensated photosynthetic downregulation in response to elevated CO_2 and warming in white birch. *Canadian Journal of Forest Research*, 52, 1176–1185.

Wang, L., Zheng, J., Wang, G. & Dang, Q.-L. (2023) Combined effects of elevated CO2 and warmer temperature on limitations to photosynthesis and carbon sequestration in yellow birch. *Tree Physiology*, 43, 379–389.

Wang, L., Zheng, J., Wang, G. & Dang, Q.-L. (2024) The combination of elevated CO_2 and warmer temperature reduces photosynthetic capacity without diluting leaf N concentration in Amur linden (*Tilia amurensis* Rupr.). *Journal of Plant Ecology*, 17(3), rtae030.

Way, D.A., Katul, G.G., Manzoni, S. & Vico, G. (2014) Increasing water use efficiency along the C3 to C4 evolutionary pathway: a stomatal optimization perspective. *Journal of Experimental Botany*, 65, 3683–3693.

Way, D.A. & Oren, R. (2010) Differential responses to changes in growth temperature between trees from different functional groups and biomes: a review and synthesis of data. *Tree Physiology*, 30, 669–688.

Way, D.A. & Sage, R.F. (2008a) Elevated growth temperatures reduce the carbon gain of black spruce [*Picea mariana* (Mill.) B.S.P.]. *Global Change Biology*, 14, 624–636.

Way, D.A. & Sage, R.F. (2008b) Thermal acclimation of photosynthesis in black spruce [*Picea mariana* (Mill.) B.S.P.]. *Plant, Cell & Environment*, 31, 1250–1262.

Way, D.A. & Yamori, W. (2014) Thermal acclimation of photosynthesis: on the importance of adjusting our definitions and accounting for thermal acclimation of respiration. *Photosynthesis Research*, 119, 89–100.

Wullschleger, S.D. (1993) Biochemical limitations to carbon assimilation in C3Plants—a retrospective analysis of the A/Ci curves from 109 species. *Journal of Experimental Botany*, 44, 907–992.

Yamori, W., Hikosaka, K. & Way, D.A. (2014) Temperature response of photosynthesis in C3, C4, and CAM plants: temperature acclimation and temperature adaptation. *Photosynthesis Research*, 119, 101–117.

Zuur, A.F., Ieno, E.N., Walker, N., Saveliev, A.A. & Smith, G.M. (2009) *Mixed effects models and extensions in ecology with R*. New York, NY: Springer.

SUPPORTING INFORMATION

Additional supporting information can be found online in the Supporting Information section at the end of this article.

How to cite this article: Dusenge, M.E., Warren, J.M., Reich, P.B., Ward, E.J., Murphy, B.K., Stefanski, A. et al. (2024) Photosynthetic capacity in middle-aged larch and spruce acclimates independently to experimental warming and elevated CO_2. *Plant, Cell & Environment*, 47, 4886–4902. https://doi.org/10.1111/pce.15068